Proceedings of the 10th World Congress on Mechanical, Chemical, and Material Engineering (MCM'24)
Barcelona, Spain - August 22-24, 2024
Paper No. ICMIE 154
DOI: 10.11159/icmie24.154

Comparative Analysis of EEG Signals in Bimanual Coordination: Real vs. Virtual Environments for Rehabilitation

Yiming Zhang[1], Jingyu Yang[1], Shijin Xu[1], Jinyuan Song[1], Zheng Yang[1], Fok Sai Cheong[1], Peng Chen[2]
[1]Sichuan University-Pittsburgh Institute,
Sichuan University Jiang'an Campus, Chengdu, China
1294120660@qq.com; 1733942830@qq.com; shijnxu26@gmail.com; 1097537934@qq.com;
zhengyang2018@scu.edu.cn; saicheong.fok@scupi.cn
[2]Southwest Jiaotong University, School of Mechanical Engineering
Southwest Jiaotong University Xipu Campus, Chengdu, China
chenpeng@swjtu.edu.cn

Abstract **-** To develop robots to assist patients in the rehabilitation of upper limbs, research into bimanual coordination is imperative. The aim of our project is to obtain, decode, and compare electroencephalogram (EEG) signals of brain activities in bimanual movement coordination in real and virtual environments. The work included the development of a virtual gaming environment for users to perform three bimanual coordination tasks. EEG signals were collected, preprocessed, and analyzed from three subjects performing these activities in the virtual environment. Time-Frequency Analysis (TFA) was used to extract features in five channels (C1, C2, C3, C4, and Cz). EEG signals were also collected from the same users performing similar activities in the real environment. Comparing the TFA results between the virtual and real environments, significant differences were found in the two subjects. Machine learning techniques were also applied to classify the three motions in the virtual and real environments based on the EEG signals collected from 64 channels. Results show that the highest average classification accuracies of 72.9 ± 9.37% and 70.5 ± 6.11% in real and virtual environments were obtained in three bimanual coordination movements using the EEGNet model. The results indicate the feasibility of decoding the bimanual coordination movements on EEG, and the impact of the virtual environment on EEG signals in time and frequency domains. In the future, we would increase the number of subjects and improve the immersion quality of our virtual environment.

Keywords**:** EEG; Virtual Reality; Time-Frequency Analysis; EEGNet; Machine Learning.

1. Introduction

Musculoskeletal disabilities are severely incapacitating and disrupt everyday activities. The World Health Organization (WHO) reports that around 1.71 billion individuals globally suffer from musculoskeletal ailments. Notable diseases impacting musculoskeletal functionality include chronic joint pain, arthritis, Parkinson's disease, and cerebral palsy [1]. Most musculoskeletal impairments experience upper extremity weakness, which prevents them from performing everyday activities with their hands [2]. It is anticipated that robots can be developed to assist physically challenged patients in performing these activities and to help in their rehabilitation. However, understanding the brain coordination of these bimanual movements is imperative for the development of the robots. According to Maiseli et al., brain-computer interfaces can accelerate the restoration of limb movement ability in disabled people, improving the condition of musculoskeletal impairments [3]. Electroencephalogram (EEG) is a non-invasive medical procedure used to record electrical activity generated in the human brain, which is one of the most frequently used methods of BCI. The principle of this technology is that nerve cells in the brain (neurons) communicate via electrical impulses, creating a pattern of electrical activity that an EEG monitor can trace [4].

Recent studies have investigated the use of virtual reality (VR) as a healthcare intervention method. For instance, in the research conducted by Jack, VR is suggested as a rehabilitative tool for stroke patients [5]; Gokeler focused on the effect of the virtual environment on the knee patterns of ACL injury patients, all of them get positive recovery in knee movement [6]; Blanco-Morab applied VR games and EEG to associate post-stroke recovery training of upper limb with bimanual motions. VR is applied as an environmental carrier, linking EEG and hand movements [7]. VR technology can provide multiple spaces and associated environmental elements compared to the real environment in a hospital [8]. Researchers can create scenarios

that are complex or difficult to reproduce in daily life using VR modelling. Switching between the scenarios makes it possible to explore how the brain responds in different mental and physiological states, thus revealing specific EEG patterns.

In summary, effective analysis of bimanual coordination from EEG signals can play an important role in development of robots and rehabilitation purposes, while the VR can help to improve the outcome of rehabilitation therapy. Hence, the aim of the project is to design EEG paradigms based on real life, obtain and decode signals of EEG in bimanual movements in both real and virtual environment. We plan to design the motor execution experiments to collect and analyse EEG data during bimanual coordination tasks to gain deeper insights into this process. To achieve this, we will establish a VR system to simulate specified bimanual coordination movements and collect EEG data within this system. After EEG data acquisition, we will preprocess the EEG data using independent component analysis (ICA) and TFA.

The paper is organized as follows: Section 2 represents the experimental paradigms, participants' information virtual environment design, and data processing including TFA and deep learning models; Section 3 discusses the experimental results from TFA and classification performance; Section 4 summarizes all the conclusions.

2. Method

2.1. Experimental Setup

Three right-handed healthy subjects participated in the experiments. All of them are male, aged between 20-22. All participants signed informed consent.

To determine paradigms for the bimanual coordinate and design tasks of movements, we could also draw inspiration from previous experimental designs [9]. Whether it is the task of opening a drawer or the coordinated movements of both hands, it can be basically summarized as the movement of both hands in the vertical and horizontal directions. This is because most bimanual movements can be simplified as the coordination movements of the two hands in these two directions. For the design of the experimental process, we aimed to make experiments effective and concise. We divided the common bimanual movements into three kinds and simplified them, and designed experiments based on these three types of movements. The design included three types of bimanual coordination: 1. horizontal movement; 2. vertical movement; 3. horizontal + vertical movement. The three movements are shown in the below diagram.

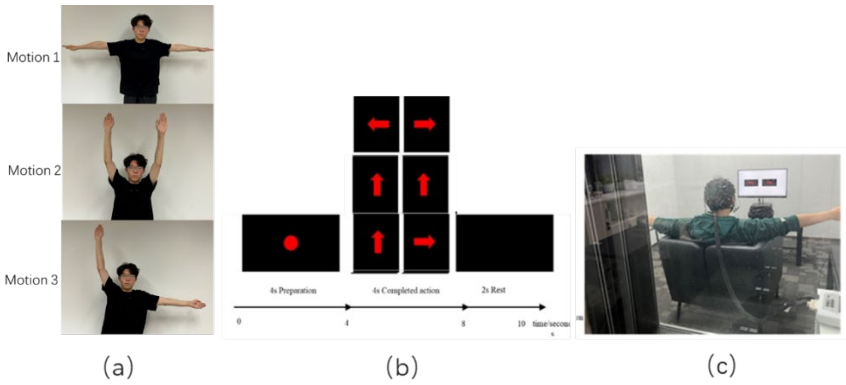

Fig. 1: Experimental setup (a) Illustration of three movements(b) Experimental process of bimanual coordination (on-screen guidance display) (c) Illustration of experiment process.

The establishment of virtual environment (VE) was based on the above designed bimanual coordination tasks in real environment. We tried to create a daily atmosphere to comfort the subjects and heighten their engagement. As a result, the virtual environment is designed to replicate the interior of a kitchen, which is shown in Fig.2 (a). The experiment takes place in the VE that was custom-made using Unity3D (editor version: 2022.3.3f1c1) and SteamVR Unity Plugin (version 2.7.3). The scenery is an open source in the asset store of unity3d, featuring a total of 78 models

including electrical appliances, kitchen tools, vases, pictures, glasses, among others, all available as prefabs. Additionally, the documentation offers various materials to customize the style of the furniture as desired.

Similar to the real environment experiments, the virtual environment uses stimulus to guide users on the bimanual activities. Arrows indicating movement directions are randomly presented in the centre of the virtual room (Fig.2 (b)). Participants perform these motions and interact with the virtual environment through a hand-held controller. Upon touching the button on the controller, visual guidance through colour changes, as well as tactile feedback through the controller ensure that the movements are properly executed.

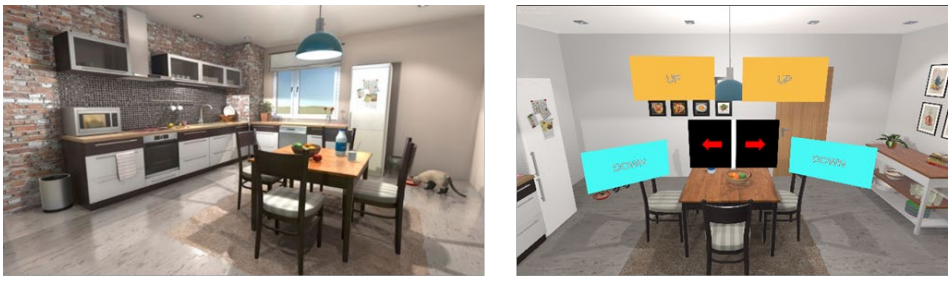

(a) (b)

Fig. 2: (a) Outline of virtual environment; (b) VR tasks.

2.2. Data Acquisition

SynAmps 2 amplifier (NeuroScan, Charlotte, NC, USA) was applied to record the EEGs using an elastic cap carrying 66 Ag/AgCl electrodes. The electrodes were placed on the scalp at locations according to the extended international 10/20 system. Electrical activities from the right and left mastoids were recorded. The vertical electrooculogram (VEOG)was recorded by bipolar channels placed above and below the left eye. The ground electrode was attached to AFz. All the electrodes were referenced to the tip of the nose. The impedances between any electrode and the reference electrode were kept at less than 5 kΩ. Continuous EEG data (0.03-100 Hz) were recorded and digitized with a 24-bit resolution with a sampling rate of 500 Hz.

2.3. Data Preprocessing

Firstly, the epoch of the actual hand movement starting from the -s to the 4s in each trial for a total of 5s was extracted from the EEG for analysis [10]. Then complete the re-reference according to the reference channels. With re-referencing, the reference channel settings can be changed to reduce or eliminate the effect of certain electrode configurations on the EEG signal [10]. Next, the EEG signal was filtered from 0.1 to 30 Hz [12].

ICA was used to remove artifacts, including eye movements, muscle activities, and external noise, thus isolating more accurate brain signals. The efficiency of ICA is influenced by several factors, such as the number of EEG channels, the experimental environment (whether stationary or mobile), and the settings of high-pass filters used in preprocessing. By enhancing the signal-to-noise ratio in specific components, ICA significantly improves the quality of EEG data, making it more suitable for detailed analysis. Furthermore, ICA's ability to distinguish between neural and non-neural signals plays a critical role in the reliability of EEG interpretations, especially in complex brain research and clinical diagnostics [13].

We implemented all the preprocessing procedures in EEGLAB, an open-source toolbox of MATLAB [14].

2.4. Decoding Model

2.4.1 Deep and Shallow ConvNet

Deep ConvNet comprises four convolutional blocks, beginning with a specially designed first block tailored for EEG input processing, followed by three conventional blocks and a layer with dense softmax classification. The first convolutional block is segmented into two layers to handle the high number of input channels. The first layer applied a temporal convolution across each filter, while the second layer conducted spatial filtering across all electrode pair combinations. The absence of

an activation function between these layers allows them to potentially be merged into a single layer. However, employing two distinct layers offers implicit regularization by separating the linear transformation into temporal and spatial components [15]. The following three blocks are conventionally used to capture the remaining features and reduce the redundant information. The illustration of Deep ConvNet architecture is shown in Fig.3 and the sizes of filter in temporal convolution and spatial filtering is set as (1,10) and (65,25).

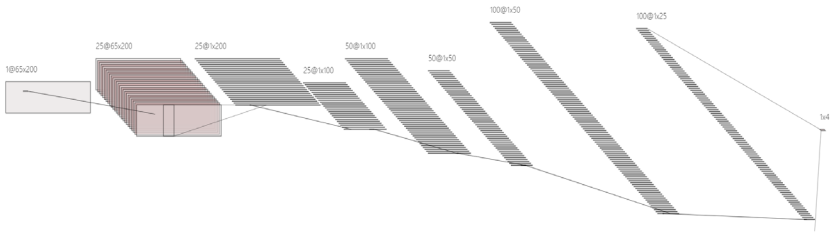

Fig. 3: The visualization of Deep ConvNet architecture

For a deeper exploration of the information in frequency band power, a shallow ConvNet is designed, drawing inspiration from the Filter Bank Common Spatial Patterns (FBCSP) algorithm [16]. The first two layers of this ConvNet comprise a temporal convolution coupled with a spatial filter. Unlike the deep ConvNet, shallow ConvNet employs a larger kernel size in the temporal convolution, enabling a larger span of transformations in this layer. After the two layers, a squaring nonlinearity, a mean pooling layer and a logarithmic activation function followed. Those two architectures have been evaluated against the conventional algorithms (FBCSP) in motor decoding from EEG [15]. With appropriate design choices, deep and shallow ConvNets are able to reach or surpass the accuracies of FBCSP and could further improved by hyperparameter optimizations.

2.4.2 EEGNet

The EEGNet architecture comprises of two main blocks. Full visualization and description of the architecture are illustrated in Table 1 and Fig. 4. Table 1 shows the network structure and training parameters for the EEGNet. In first block, it has two convolutional steps. First, 2D convolutional filters of size (1, 250) are utilized. The length of these filter is half the sampling rate of the data (500 Hz), enabling the capture of frequency information at 2 Hz and above [17]. The batch normalizations follow to optimize the output activations. Then a depthwise convolution layer of size (65, 1) is applied to learn a spatial filter. This step improves the learning of spatial filters corresponding to each temporal filter, while enhancing the extraction of frequency-specific spatial features [17]. Depth parameter D controls the number of spatial filters.

To combine the features from the previous output, a separable convolution is used in block2. It consists of a depthwise convolution of size (1, 50), followed by F2 (1, 1) pointwise convolutions. The depthwise convolution summarizes the individual feature maps in time and the pointwise convolution capture new features by mixing the resulting output channels of feature maps [18]. This step is beneficial for EEG signals since distinct feature maps can encode data across various temporal scales of information.

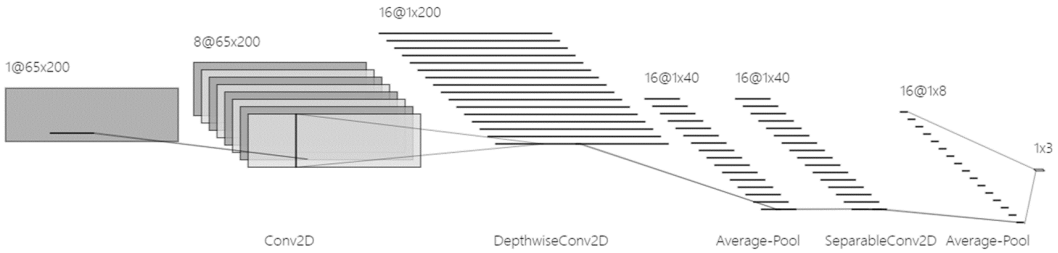

Fig. 4: Illustration of the EEGNet architecture. Conv2D is applied as a temporal layer to learn the frequency features, Depthwise convolution is followed to learn the spatial features. Then separable convolution summarizes the temporal features for each map [17]

Table 1: The network structure and training parameters of EEGNet. T is the number of sample points, C is the number of EEG channels, F_1 is the number of temporal filters and F_2 is the pointwise filters

Block	Layer	Filter number	Kernel size	Output	Activation	Options
1	Input			(C,T)		
	Reshape			$(1,\mathrm{C},\mathrm{T})$		
	Conv2D	F_1	(1,250)	$(F_1,\mathrm{C},\mathrm{T})$	Linear	Mode = same
	BatchNorm			$(F_1,\mathrm{C},\mathrm{T})$		
	DepthwiseConv2D	$D * F_1$	(65,1)	$(\mathrm{D} * F_1,\mathrm{C},\mathrm{T})$	Linear	Mode = valid
	BatchNorm			$(\mathrm{D} * F_1,\mathrm{C},\mathrm{T})$		
	Activation			$(\mathrm{D} * F_1,\mathrm{C},\mathrm{T})$		
	AveragePool2D		(1,5)	$(\mathrm{D} * F_1,\mathrm{C},\mathrm{T}//5)$	ELU	
	Dropout			$(\mathrm{D} * F_1,\mathrm{C},\mathrm{T}//5)$		$\mathrm{p} = 0.5$
2	SeparableConv2D	F_2	(1,50)	$(F_2,C,T//5)$	Linear	Mode = same
	BatchNorm			$(F_2,C,T//5)$		
	Activation			$(F_2,C,T//5)$	ELU	
	AveragePool2D		(1,5)	$(F_2,C,T//25)$		
	Dropout			$(F_2,C,T//25)$		$\mathrm{p} = 0.5$
	Flatten			$(F_2,C,T//25)$		
Classifier	Dense				Softmax	Max norm=0.25

2.4.3 Training Strategy

EEG signals collected in the virtual environment by ME and the real environment by IE were processed into a uniform size (150,2500,65). Before we applied the proposed methods, the input data were reshaped. Three-dimensional data of form $(\mathrm{N_s},\mathrm{L},\mathrm{N_c})$ was transformed into four dimensions $(1,\mathrm{N_s},\mathrm{T},\mathrm{C})$, where $\mathrm{N_s}$ is the number of input samples and T is the number of sample points and $\mathrm{N_c}$ is the number of EEG channels. To ensure the reliability of the model performance, we applied the 10-fold cross-validation to split the dataset into 10 groups. Each group would be used for testing and the remaining nine groups were used as training sets. Therefore, 10 models would be trained for one time and the average accuracy of the models represents the performance of the algorithm. We applied the adaptive moment estimation (Adam) as the optimizer and categorical cross-entropy for multi-classification loss function. To optimize the models, we set a grid of hyperparameters such as epoch in [100,150,200,250,300], number of filters (from 4 to 19) and batch size in [8,16,32,64]. The settings of hyperparameters are chosen based on the highest average accuracy.

3. Results

3.1 Time-frequency Presentation

For TFA, we primarily analyzed the results of data from the C1, C2, C3, C4, and Cz channels. Since the results of the five channels were similar, only the results of the C1 channel are presented [19] [20]. The results in the time domain showed that the peak of Movement 1 is often significantly lower than the other two movements. On this basis, we used the Morlet

wavelet transform to calculate the time-frequency representation for further analysis of the results. Meanwhile, we plotted the time-frequency diagram based on this result which is shown in Fig.5.

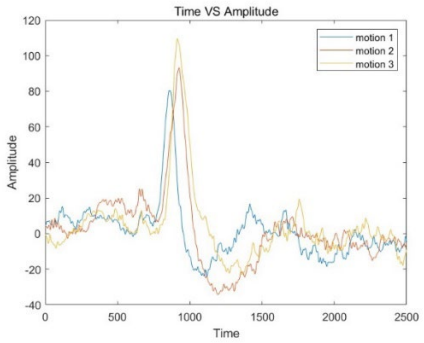

Fig. 5: Average Amplitude vs Time diagram of C1 channel under three different movements conditions

Based on these time-frequency diagrams, we can find that with five of our selected channels, C1, C2, C3, C4, and Cz, the three types of bimanual coordination movements we have designed show more pronounced energy concentrations mainly in the frequency domain from 2 to 12 Hz, and that some of the channels will have energy concentrations below 2 Hz. Therefore, from the results of analysing the time-frequency diagrams of the five channels of data, C1, C2, C3, C4, and Cz, it is difficult to distinguish between the three kinds of movements just by these energy concentrations in experiments conducted in a VR environment. Time-frequency diagrams are difficult to use as a decisive basis for distinguishing between the three movements, because it is difficult to directly identify the differences and distinctions between the three based on the images.

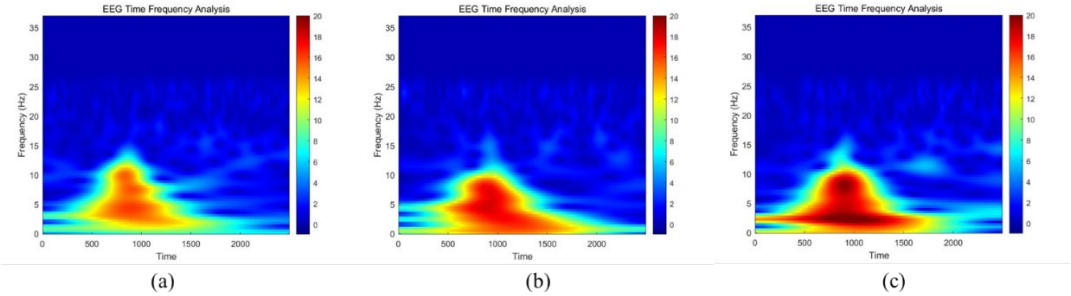

Fig. 6: Time-frequency diagrams of C1channels for three movements. From left to right column, (a) movement 1, (b) movement 2, and (c) movement 3.

3.2 Decoding Performance

Furthermore, we compared the performance of the three deep learning methods--EEGNet, Shallow convolution network and deep convolution network. All models are trained in the same way. The results of three subjects are shown in Table 2. It could be seen that EEGNet performs better than other two algorithms of all subjects. (a) represents the visualization of three algorithms in Subject 2. Besides, we applied t-test to determine whether the accuracies have significant difference between the virtual and real environment. We found that subjects get higher accuracy in virtual environment in EEGNet except Subject 3, which supports the results in Table 2. The visualization of the classification accuracies is shown in Fig. 7(b). Hence, the classification accuracies in virtual environment are comparable to the real environment.

Table 2: Accuracies of classification for three movements using three algorithms

Subject	Environment	EEGNet	ShallowConvNet	DeepConvNet
Subject 1	VR	0.87	0.62	0.75
	Real	0.71	0.48	0.54
Subject 2	VR	0.83	0.58	0.87

Subject 3	Real	0.72	0.43	0.46
	VR	0.58	0.38	0.50
	Real	0.71	0.60	0.60

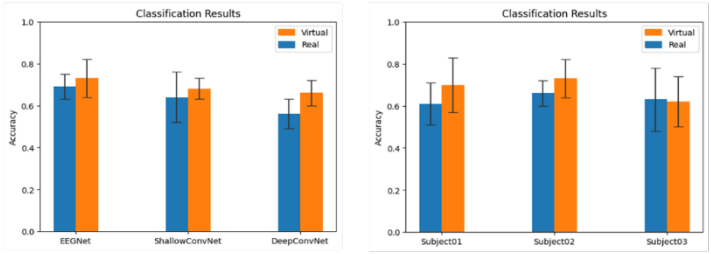

(a) (b)

Fig. 7: (a) Classification Results of Three Algorithms (Subject 2) (b) Classification Results of Three Subjects in Real and Virtual Environment using EEGNet

4. Conclusion

Bimanual coordination is significantly important in various aspects of daily life. In our project, we collected the EEG data during the experiment of three types of bimanual coordination movements including: horizontal movement, vertical + horizontal movement, and vertical movement using experiments in the virtual environment. The results were compared with similar experiments with subjects in the real environment conducted by IE students.

Based on the results of TFA time-amplitude diagram, motion 1 is more likely to be distinguished from the other two motions for two subjects. The peak voltage of motion1 is lower in Subject 1 and Subject 2. Our results correspond to the IE report that the binary classification of Motion 1 and Motion 2 is the highest in Subject 1 and Subject 2, which means the differences between these two types of motion are the biggest. The result of the TFA is that under the five channels C1, C2, C3, C4, and Cz, only Motion 1 and 2 of Subject 1 can be seen to differ by the time-frequency diagrams in the REAL environment. By significance analysis, only the three movements of Subject 1 in the VR environment showed more significant differences. However, the significance of the differences between the three movements of Subject 1 and Subject 2 in the VR environment was higher than that in the REAL environment.

The results of EEG decoding show that the EEG signals of the three movements can be decoded by the three deep learning algorithms and the highest average classification accuracies in subjects are $72.9 \pm 9.37\%$ and $70.5 \pm 6.11\%$ in real and virtual environments. We compare the decoding performances in real and virtual environments. Average accuracies in the virtual environment are higher than that in the real environment (except Subject 3), which shows that the decoding results in virtual environment are comparable to the real environment. In addition, the performances of EEGNet model are more successful than the other two models, Deep and shallow ConvNet.

However, our work still has several limitations. First, the number of subjects was too small and the amount of data was small. Since the experiment had only three subjects and all three subjects were healthy males in their 20s, the conclusions drawn may not be generalizable. Considering that the goal of this project was to be used for exercise rehabilitation, there is no data from patients to compare with data from healthy subjects.

Second, the EEG cap used during EEG data acquisition has 65 channels. By reading the literature, we focused on the data of 5 channels, C1, C2, C3, C4, and Cz. Due to time constraints, we did not analyze the remaining channels in detail. There may exist other channels that have a more significant effect on the bimanual coordination movement, or can better respond to the results of two-handed movement.

Third, the designed virtual environment is monotonous and not immersive. A great virtual environment has no distinction from the real environment and can make users immersive. However, the VR headset is unused during our experiments. The reason is that the data quality on EEG cap will be affected by the headset while wearing both of them. Meanwhile, long time of wearing the headset will cause dizziness and make subjects uncomfortable. In addition, the virtual scenario is too simple. Different scenarios might affect the brain activity and change the patterns in EEG signals.

Acknowledgements

We would like to express our sincere gratitude to our advisors, professors Zheng Yang, Sai Cheong Fok and Peng Chen. Their invaluable guidance, insightful critiques and encouragement are crucial in the development of this project. Their feedback and suggestions are immensely helpful in shaping the direction and execution of our research. We would also like to thank professors Peng Chen, Rong Yin, Feng Gu and their student teams for their collaboration and supports on data collection.

References

[1] T. Rose, C. S. Nam, and K. B. Chen, "Immersion of virtual reality for rehabilitation - Review," Applied Ergonomics, vol. 69, pp. 153–161, May 2018, doi: 10.1016/j.apergo.2018.01.009.

[2] V. Rajendran, D. Jeevanantham, C. Larivière, R.-J. Singh, L. Zeman, and P. Papuri, "Effectiveness of self-administered mirror therapy on upper extremity impairments and function of acute stroke patients: study protocol," Trials, vol. 22, no. 1, p. 439, Jul. 2021, doi: 10.1186/s13063-021-05380-9.

[3] B. Maiseli, A. T. Abdalla, L. V. Massawe, M. Mbise, K. Mkocha, N. A. Nassor, M. Ismail, J. Michael, S. Kimambo., "Brain–computer interface: trend, challenges, and threats," Brain Inf., vol. 10, no. 1, p. 20, Aug. 2023, doi: 10.1186/s40708-023-00199-3.

[4] M. Teplan, "FUNDAMENTALS OF EEG MEASUREMENT," MEASUREMENT SCIENCE REVIEW, vol. 2, 2002.

[5] D. Jack, R. Boian, A. S. Merians, M. Tremaine, G. C. Burdea, S. V. Adamovich, M. Recce, H. Poizner, "Virtual reality-enhanced stroke rehabilitation," IEEE Transactions on Neural Systems and Rehabilitation Engineering, vol. 9, no. 3, pp. 308–318, Sep. 2001, doi: 10.1109/7333.948460.

[6] A. Gokeler, M. Bisschop, G. D. Myer, A. Benjaminse, P. U. Dijkstra, H. G. van keeken, J. J. van Raay, J. G. Burgerhof, E. Otten, "Immersive virtual reality improves movement patterns in patients after ACL reconstruction: implications for enhanced criteria-based return-to-sport rehabilitation," Knee Surg Sports Traumatol Arthrosc, vol. 24, no. 7, pp. 2280–2286, Jul. 2016, doi: 10.1007/s00167-014-3374-x.

[7] D. A. Blanco-Mora, Y. Almeida, C. Vieira, and S. B. i Badia, "A Study on EEG Power and Connectivity in a Virtual Reality Bimanual Rehabilitation Training System," in 2019 IEEE International Conference on Systems, Man and Cybernetics (SMC), Oct. 2019, pp. 2818–2822. doi: 10.1109/SMC.2019.8914190.

[8] I. A. Castiblanco Jimenez, F. Marcolin, L. Ulrich, S. Moos, E. Vezzetti, and S. Tornincasa, "Interpreting Emotions with EEG: An Experimental Study with Chromatic Variation in VR," in Advances on Mechanics, Design Engineering and Manufacturing IV, S. Gerbino, A. Lanzotti, M. Martorelli, R. Mirálbes Buil, C. Rizzi, and L. Roucoules, Eds., Cham: Springer International Publishing, 2023, pp. 318–329. doi: 10.1007/978-3-031-15928-2_28.

[9] S. J. Xu, J. Y. Song, Y. M. Zhang, J. Y. Yang, Z. Yang, F. S. Cheong, P. Chen, "Topological Data Analysis and Decoding Based on Electroencephalogram Signals", preprint.

[10] M. X. Cohen, "Analyzing neural time series data: Theory and practice".

[11] A. Delorme, "EEG is better left alone," Sci Rep, vol. 13, no. 1, p. 2372, Feb. 2023, doi: 10.1038/s41598-023-27528-0.

[12] L. Hu and Z. Zhang, Eds., EEG Signal Processing and Feature Extraction. Singapore: Springer Singapore, 2019. doi: 10.1007/978-981-13-9113-2.

[13] M. Klug and K. Gramann, "Identifying key factors for improving ICA-based decomposition of EEG data in mobile and stationary experiments," European Journal of Neuroscience, vol. 54, no. 12, pp. 8406–8420, 2021, doi: 10.1111/ejn.14992.

[14] A. Delorme and S. Makeig, "EEGLAB: an open source toolbox for analysis of single-trial EEG dynamics including independent component analysis," Journal of Neuroscience Methods, vol. 134, no. 1, pp. 9–21, Mar. 2004, doi: 10.1016/j.jneumeth.2003.10.009.

[15] R. T. Canolty, E. Edwards, S. S. Dalal, M. Soltani, S. S. Nagarajan, H. E. Kirsch, M. S. Berger, N. M. Barbaro, R. T. Knight, "High Gamma Power Is Phase-Locked to Theta Oscillations in Human Neocortex," Science (New York, N.Y.), vol. 313, no. 5793, p. 1626, Sep. 2006, doi: 10.1126/science.1128115.

[16] R. T. Schirrmeister, J. T. Springenberg, L. D. J. Fiederer, M. Glasstetter, K. Eggensperger, M. Tangermann, F. Hutter, W. Burgard, T. Ball, "Deep learning with convolutional neural networks for EEG decoding and visualization," Human Brain Mapping, vol. 38, no. 11, pp. 5391–5420, 2017, doi: 10.1002/hbm.23730.
[17] F. Chollet, "Xception: Deep Learning with Depthwise Separable Convolutions," in 2017 IEEE Conference on Computer Vision and Pattern Recognition (CVPR), Honolulu, HI: IEEE, Jul. 2017, pp. 1800–1807. doi: 10.1109/CVPR.2017.195.
[18] V. J. Lawhern, A. J. Solon, N. R. Waytowich, S. M. Gordon, C. P. Hung, and B. J. Lance, "EEGNet: A Compact Convolutional Network for EEG-based Brain-Computer Interfaces," J. Neural Eng., vol. 15, no. 5, p. 056013, Oct. 2018, doi: 10.1088/1741-2552/aace8c.
[19] M. Zhang, J. Wu, J. Song, R. Fu, R. Ma, Y. C. Jiang, Y. F. Chen, "Decoding Coordinated Directions of Bimanual Movements From EEG Signals," IEEE Trans. Neural Syst. Rehabil. Eng., vol. 31, pp. 248–259, 2023, doi: 10.1109/TNSRE.2022.3220884.
[20] H. Li, G. Huang, Q. Lin, J. Zhao, Q. Fu, L. Li, Y. Mao, X. Wei, W. Yang, B. Wang, Z. Zhang, "EEG Changes in Time and Time-Frequency Domain During Movement Preparation and Execution in Stroke Patients," Front. Neurosci., vol. 14, Aug. 2020, doi: 10.3389/fnins.2020.00827.